

The Load-Modulated Linearizer: A Technique for Intermodulation Cancellation in PA Systems

Anton N. Atanasov^{#1}, Wasam R. A. Mukhtar Ahmad [#], Mark S. Oude Alink[#], Frank E. van Vliet^{*#}

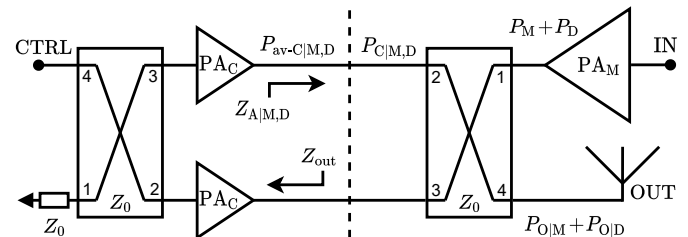
[#]Integrated Circuit Design, University of Twente, Enschede, Netherlands

*Defence, Safety & Security, TNO, The Hague, Netherlands

¹a.n.atanasov@utwente.nl

Keywords—intermodulation, linearization, load-modulation, power amplifiers, compression, nonlinearity, 5G, LMBA.

I. INTRODUCTION



$$Z_{A|M,D} = Z_0 \left(1 + \sqrt{2} \frac{I_{M,D}}{I_{C,M,D} e^{j\phi}} \right) = \begin{cases} Z_{out}^* & \text{for } P_M \\ -Z_0 & \text{for } P_D, \end{cases} \quad (1)$$

where $I_{M,D}$ is the set of all currents, main and distortion, coming from the PA_M and $I_{C,M,D} e^{j\theta}$ is the set of all complex control currents coming from the control PAs [7]. The set of phases, ϕ , allow $Z_{A|M,D}$ to achieve the required values. Under these conditions the sum total output power at the antenna port across the full spectrum of the LML becomes

$$P_{O|M} = 2P_{C|M} + P_M = 2 \frac{P_M}{\alpha_M} + P_M = \left(\frac{2 + \alpha_M}{\alpha_M} \right) P_M \quad (2)$$

$$P_{O|D} = 2P_{C|D} + P_D = 2 \frac{P_D}{\alpha_D} + P_D = 0,$$

where $P_{C|M}$ and $P_{C|D}$ are the sum total of all individual control powers delivered by a single control device in order to couple P_M and absorb P_D , respectively. The control signal power (CSP) factors α_M and α_D describe how these powers govern the load-modulated drive impedances $Z_{A|M}$ and $Z_{A|D}$, respectively. The two CSP factors define circular impedance contours on the Smith chart and are chosen such that both coupling and absorbing is achieved using the least amount of total control power

$$\alpha_{M,D} = \frac{P_{M,D}}{P_{C|M,D}} = \frac{|Z_{A|M,D}/Z_0 - 1|^2}{2\text{Re}\{Z_{A|M,D}/Z_0\}} = \begin{cases} 2\sqrt{\frac{P_M}{P_D}} & \text{for } P_M \\ -2 & \text{for } P_D. \end{cases} \quad (3)$$

The active load-modulated $Z_{A|M,D}$ impedances affect how much of the control PA's available powers, $P_{av-C|M,D}$, enter the output hybrid coupler

$$P_{C|M,D} = P_{av-C|M,D} (1 - |\Gamma_{A|M,D}|^2), \quad (4)$$

where $|\Gamma_{A|M,D}|^2$ are the drive impedance reflection coefficients from the control PA's perspective. When coupling the main powers, $|\Gamma_{A|M}|^2$ becomes 0 and all the control power is recovered at the antenna port, as with the LMBA [7]. When absorbing the distortion tones, $|\Gamma_{A|D}|^2$ is chosen such that it minimizes the total available control power used

$$|\Gamma_{A|M,D}|^2 = \left| \frac{Z_{A|M,D} - Z_{out}}{Z_{A|M,D} + Z_{out}} \right|^2 = \begin{cases} 0 & \text{for } P_M \\ \sqrt{\frac{P_D}{P_M}} + 1 & \text{for } P_D. \end{cases} \quad (5)$$

Absorbing power ($\alpha_D = -2$) means that $P_{av-C|D} > 0$, which follows from (4) with $P_{C|D} < 0$ and $|\Gamma_{A|D}|^2 > 1$. The coupling and absorbing mechanisms oppose each other with respect to choice of Z_{out} . Any improvement in one incurs a corresponding power penalty on the other.

The relationship between P_M and P_D for a PA_M , at a given bias point, determines the balance between $P_{av-C|M}$ and $P_{av-C|D}$, such that the minimum total available control power, P_{T-min} , from a single control device is

$$P_{T-min} = \sqrt{P_M P_D}, \quad (6)$$

which is simply the geometric mean between the total wanted and unwanted power levels at the output of PA_M . Thus, P_M and P_D uniquely determine the Z_{out} at which coupling and absorbing can be achieved using the least available total control power. Consequently, P_T is smallest when $P_{av-C|M} = P_{av-C|D}$.

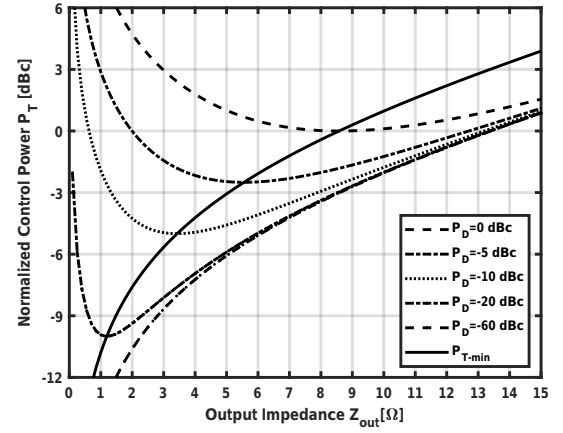


Fig. 2. Total relative available control power, P_T , from a single control PA for different amounts of distortion power, P_D , relative to a reference P_M (0 dBc) as a function of Z_{out} with $Z_0 = 50\Omega$ from an arbitrary PA_M . The P_T curve shows the minimum control power for a given Z_{out} .

Figure 2 shows the relative total control power needed to couple a reference P_M power and absorb several P_D powers of varying strength in a 50Ω environment as a function of Z_{out} . A perfectly linear PA_M requires no control power as Z_{out} can be set to a complete short circuit (or open), reflecting all power towards the output. As Z_{out} converges to Z_0 , absorbing P_D requires less power but the cost of coupling P_M increases. Additionally, P_T is more susceptible to variations in P_D at lower Z_{out} values than at higher ones. The optimal Z_{out} is defined as

$$Z_{out} = Z_0 \frac{1 - \sqrt{\frac{\alpha_M}{2 + \alpha_M}}}{1 + \sqrt{\frac{\alpha_M}{2 + \alpha_M}}}. \quad (7)$$

The efficiency of the LML, η_{LML} , is defined as the ratio between useful output RF power, P_{RFout} , and total DC power, $P_{DCtotal}$. Using (3) and (6) η_{LML} can be calculated as

$$\eta_{LML} = \frac{P_{RFout}}{P_{DCtotal}} = \frac{(P_M + P_T) \eta_M \eta_C}{(P_M + P_D) \eta_C + 2P_T \eta_M}, \quad (8)$$

where η_M and η_C are the amplifier efficiencies [16] of the main and control PAs, respectively. In a real system, the control PAs will be sized according to the necessary power for the LML to work at sufficient linearity. Therefore, they are likely to be less efficient than the main PA operating in compression.

For example, if $\eta_M = 50\%$, $\eta_C = 25\%$, $P_M = 0\text{dBc}$ and $P_D = -20\text{dBc}$, then the total efficiency would only decrease to 39% over a wide range of P_D for configurations where $\eta_C \leq \eta_M$, as shown in Fig. 3. The peak efficiency of the system is achieved when the least amount of P_T is used to achieve both coupling and absorption. The LML is fully defined by

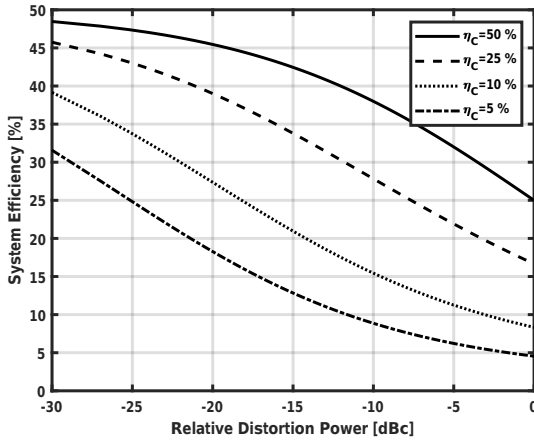


Fig. 3. Total system efficiency as function of increasing relative distortion power P_D in dBc for several control PA efficiencies. The main Pa's efficiency is fixed at $\eta_M = 50\%$.

P_M and P_D and remains power efficient at high compression levels due to the small P_T needed.

III. LOAD-MODULATED LINEARIZER PROTOTYPE

The LML measurement setup was constructed using three identical commercial PAs (ZRL-2400LN+, 1 – 2.4GHz) with input-related $P_{1dB} = -9dBm$ and $P_{3dB} = -7dBm$. Their main tone inputs, at $\approx 2GHz$, are generated using two signal generators and the coupling and absorbing control tones are generated using six separate signal generators, as shown in Fig. 4 where the main and control signals are represented by a single piece of equipment for clarity. Wilkinson combiners (ZN2PD2-63-S+, 0.35 – 6GHz) are used to guarantee 20dB of isolation between the generators. The Z_{out} of the two control PAs was set to 8Ω ($\alpha_M \approx 2.2$) using a pair of custom PCB-based quarter-wave transformers. The combiners and the quadrature hybrid couplers have an insertion loss of approximately 0.9dB each; these losses were compensated for in the generation.

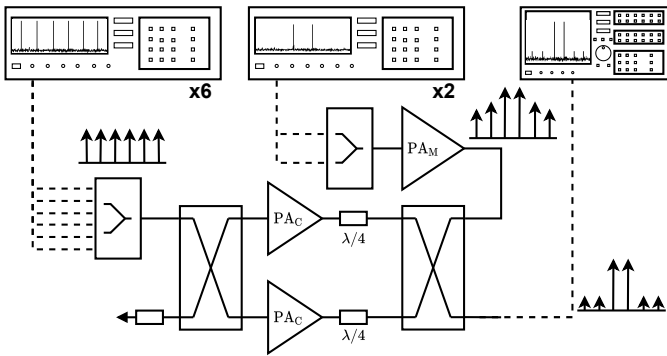
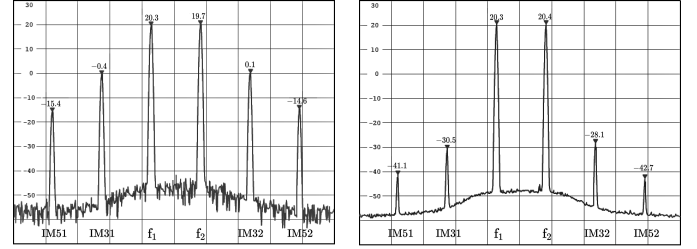


Fig. 4. Measurement setup of LML. The two coupling and four absorbing tones are generated separately using six signal generators on the control side and the two main input tones are generated 100KHz apart on the PA_M side using two signal generators.

The PA_M is driven at its P_{3dB} compression point by two tones 100kHz apart, producing two main tones as well as

unwanted IMD tones. The LML uses six separate signal generators to create the two coupling and four absorbing tones that feed into the control PAs. Once the amplitude of each control tone is evaluated, they are individually phase-shifted until the desired effect is achieved. To achieve a suppression of 30dB requires a phase accuracy of ± 2 degrees and an amplitude accuracy of $\pm 0.5dB$.



(a) Output spectrum of the PA_M . (b) Output spectrum of the LML. Fig. 5. Performance of the LML in linearising a PA operating at P_{3dB} .

Fig. 5a) shows the output spectrum of the PA_M amplifying two main tones at its P_{3dB} compression point. In Fig. 5b) an overall IMD suppression of about 30dB is measured, while coupling the main tones and their control tones at the output. The slight increase in $P_{O|M}$ comes from the contribution of the control tones due to α_M . As an added benefit, tones that are not actively absorbed, such as IM7 and higher order ones, experience a passive attenuation of about 3dB, due to $Z_{out} = 8\Omega$, when they reach the antenna port.

IV. BENCHMARKING THE LML VS DPD

We compare the LML to the simplest form of DPD, implemented as shown in Fig. 6. Two main tones and two IM3 correction tones are generated and combined in the same way as with the LML and are applied to the same PA_M .

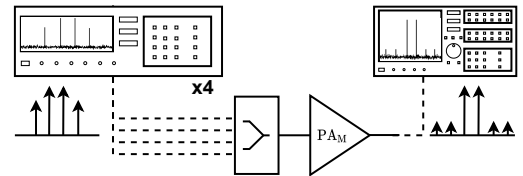


Fig. 6. Measurement setup of DPD with two main tones and two correction tones generated 100KHz apart.

The output power of the LML and DPD systems is compared to that of the main PA's P_M as a function of input power and the results are shown in Figs. 7a) and b). The LML maintains a constant power increase over PA_M due to the contribution of the control PAs, whereas the DPD system, due to its different nature, incurs a certain power cost from the correction tones. The LML does not restrict the output power as the input power is increased past the P_{1dB} compression point. On the other hand, the DPD system causes an eventual gain compression as suppressing the growing IM3 products requires a corresponding power increase in the correction tones.

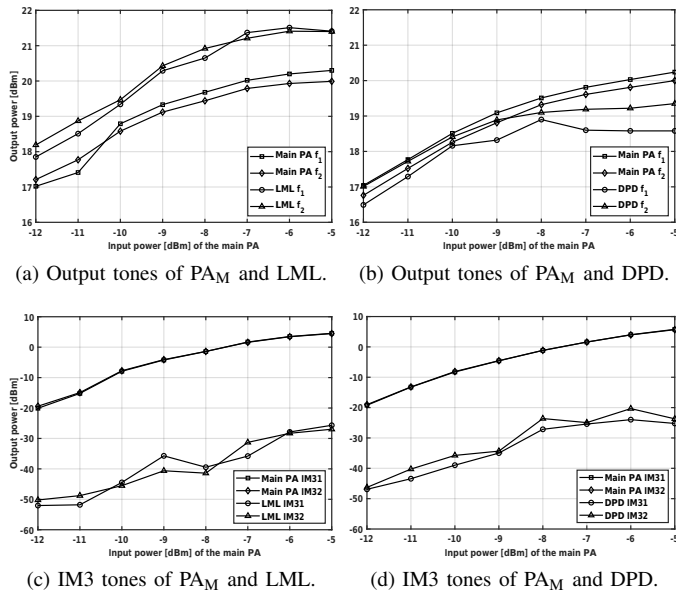


Fig. 7. Output power of LML and DPD systems relative to PA_M 's output power for a range of input powers.

In a similar manner, the suppression of the IM3 tones is compared between the LML and DPD in Figs. 7c) and d). Both the LML and DPD are about equally sensitive to amplitude and phase errors in the control and correction tones, respectively, but the LML does not influence the behaviour of IMD the same way DPD does. The two systems are able to suppress the IM3 tones equally well, however, the LML can selectively absorb individual unwanted tones and requires simpler control signals, which also simplifies the necessary control scheme.

V. CONCLUSION

The LML is a novel AM/AM PA linearization system for simultaneous multi-beam active array transmitters using active load-modulation based on the LMBA which is capable of coupling wanted tones to the output and selectively absorbing unwanted ones. It combines the power conservation properties of the LMBA with the ability to linearize at a very low power and complexity penalty. The LML operates at the main PA's output and it neither influences the IMD mechanisms, nor does it constrain the output power like DPD does. The system achieves IMD suppression of about 30dB, while the main PA operates at P_{3dB} compression point and above, with a phase and amplitude error tolerance of ± 2 degrees and ± 0.5 dB, respectively. Additionally, IMD components not load-modulated by the LML are passively attenuated due to the mismatch between Z_{out} and Z_0 . When the main PA is in OBO it was shown that the LML achieves similar IMD suppression as DPD, making it a suitable complement to existing DPD systems.

REFERENCES

- [1] F. Raab, P. Asbeck, S. Cripps, P. Kenington, Z. Popovic, N. Potheary, J. Sevic, and N. Sokal, "Power Amplifiers and Transmitters for RF and Microwave," *IEEE Transactions on Microwave Theory and Techniques*, vol. 50, no. 3, pp. 814–826, 2002.
- [2] A. Katz, J. Wood, and D. Chokola, "The Evolution of PA Linearization: From Classic Feedforward and Feedback Through Analog and Digital Predistortion," *IEEE Microwave Magazine*, vol. 17, no. 2, pp. 32–40, 2016.
- [3] F. H. Raab, "Efficiency of Doherty RF Power-Amplifier Systems," *IEEE Transactions on Broadcasting*, vol. BC-33, no. 3, pp. 77–83, 1987.
- [4] J. Zanen, E. Klumperink, and B. Nauta, "Power Efficiency Model for MIMO Transmitters Including Memory Polynomial Digital Predistortion," *IEEE Transactions on Circuits and Systems II: Express Briefs*, vol. 68, no. 4, pp. 1183–1187, 2021.
- [5] W. Sandrin, "Spatial Distribution of Intermodulation Products in Active Phased Array Antennas," *IEEE Transactions on Antennas and Propagation*, vol. 21, no. 6, pp. 864–868, 1973.
- [6] C. Hemmi, "Pattern Characteristics of Harmonic and Intermodulation Products in Broadband Active Transmit Arrays," *IEEE Transactions on Antennas and Propagation*, vol. 50, no. 6, pp. 858–865, 2002.
- [7] D. J. Sheppard, J. Powell, and S. C. Cripps, "An Efficient Broadband Reconfigurable Power Amplifier Using Active Load Modulation," *IEEE Microwave and Wireless Components Letters*, vol. 26, no. 6, pp. 443–445, 2016.
- [8] P. H. Pednekar and T. W. Barton, "RF-input Load Modulated Balanced Amplifier," in *2017 IEEE MTT-S International Microwave Symposium (IMS)*, 2017, pp. 1730–1733.
- [9] R. Quaglia and S. Cripps, "A Load Modulated Balanced Amplifier for Telecom Applications," *IEEE Transactions on Microwave Theory and Techniques*, vol. 66, no. 3, pp. 1328–1338, 2018.
- [10] M. Faulkner, "Amplifier Linearization Using RF Feedback and Feedforward Techniques," *IEEE Transactions on Vehicular Technology*, vol. 47, no. 1, pp. 209–215, 1998.
- [11] A. Katz, R. Sudarsanam, and D. Aubert, "A Reflective Diode Linearizer for Spacecraft Applications," in *1985 IEEE MTT-S International Microwave Symposium Digest*, 1985, pp. 661–664.
- [12] G. C. Tripathi and M. Rawat, "Predistortion Linearizer Design for Ku-Band RF Power Amplifier," in *2019 National Conference on Communications (NCC)*, 2019, pp. 1–6.
- [13] M. P. Nathalie Deltimple, Anthony Ghiotto, "Fully Integrated Reflector-Based Analog Predistortion for Ku-Band Power Amplifiers Linearization," in *ESSCIRC ESSDERC 2021*, 2021.
- [14] V. Qunaj and P. Reynaert, "A Ka-Band Doherty-Like LMBA for High-Speed Wireless Communication in 28-nm CMOS," *IEEE Journal of Solid-State Circuits*, vol. 56, no. 12, pp. 3694–3703, 2021.
- [15] Y. Cao and K. Chen, "Pseudo-Doherty Load-Modulated Balanced Amplifier with Wide Bandwidth and Extended Power Back-Off Range," *IEEE Transactions on Microwave Theory and Techniques*, vol. 68, no. 7, pp. 3172–3183, 2020.
- [16] B. Kim, "Chapter 2 - Power Amplifier Fundamentals," in *RF and mm-Wave Power Generation in Silicon*, H. Wang and K. Sengupta, Eds. Oxford: Academic Press, 2016, pp. 17–58.